

Lawrence Berkeley National Laboratory

LBL Publications

Title

The potential of bacterial microcompartment architectures for phytonanotechnology

Permalink

<https://escholarship.org/uc/item/57g585tx>

Journal

Environmental Microbiology Reports, 14(5)

ISSN

1758-2229

Authors

Raba, Daniel A

Kerfeld, Cheryl A

Publication Date

2022-10-01

DOI

10.1111/1758-2229.13104

Copyright Information

This work is made available under the terms of a Creative Commons Attribution License, available at <https://creativecommons.org/licenses/by/4.0/>

Peer reviewed

1 **The Potential of Bacterial Microcompartment Architectures for Phytonanotechnology**

2

3 **Daniel A Raba^a and Cheryl A Kerfeld^{abc}**

4

5 ^a MSU-DOE Plant Research Laboratory, Michigan State University, 612 Wilson Road, East
6 Lansing, MI 48824, USA

7 ^b Environmental Genomics and Systems Biology and Molecular Biophysics and Integrated
8 Bioimaging Divisions, Lawrence Berkeley National Laboratory, 1 Cyclotron Road, Berkeley, CA
9 94720, USA

10 ^c Department of Biochemistry and Molecular Biology, Michigan State University, 603 Wilson
11 Road, East Lansing, MI 48824, USA

12

13 **Summary**

14 The application of nanotechnology to plants, termed phytonanotechnology, has the potential to
15 revolutionize plant research and agricultural production. Advancements in phytonanotechnology will
16 allow for the time-controlled and target-specific release of bioactive compounds and agrochemicals to
17 alter and optimize conventional plant production systems. A diverse range of engineered nanoparticles
18 with unique physiochemical properties are currently being investigated to determine their suitability for
19 plants. Improvements in crop yield, disease resistance, and nutrient and pesticide management are all
20 possible using designed nanocarriers. However, despite these prospective benefits, research to
21 thoroughly understand the precise activity, localization, and potential phytotoxicity of these
22 nanoparticles within plant systems is required. Protein-based bacterial microcompartment shell proteins
23 that self-assemble into spherical shells, nanotubes, and sheets, could be of immense value for
24 phytonanotechnology due to their ease of manipulation, multifunctionality, rapid and efficient
25 producibility, and biodegradability. In this review, we explore bacterial microcompartment-based
26 architectures within the scope of phytonanotechnology.

27

28 **Introduction**

29 The field of phytonanotechnology is a new and promising area of research that involves the use
30 of engineered nanoparticles (ENPs) to alter and/or enhance conventional plant systems (Hatami *et al.*,
31 2016; Wang *et al.*, 2016; Rodrigues *et al.*, 2017; Shang *et al.*, 2019; Jiang *et al.*, 2021; Agrawal *et al.*,
32 2022). Through “on-demand” and “on-command” targeted delivery of bioactive molecules and
33 agrochemicals, ENPs could have an immense impact on significant global problems related to climate
34 change and the scale of food production (Nair *et al.*, 2010). ENPs in phytonanotechnology are designed
35 with key physiochemical features such as programmable surface area, highly-charged surface potential,
36 enhanced reactivity, cargo binding domains, etc. that provide functionality as nanocarriers within plants
37 (Cunningham *et al.*, 2018; Demirer *et al.*, 2019). These properties are dependent on the chemical
38 composition, surface structure, size, morphology, and solubility (Wong *et al.*, 2016; Vega-Vásquez *et al.*,
39 2020). The surge in the use of nanoparticles in medicine and material fabrication has led to the
40 advancement of novel medical therapies and industrial products that include microelectronics,
41 semiconductors, catalysts and household products (Smith *et al.*, 2013; Neupane *et al.*, 2019; Vega-
42 Vásquez *et al.*, 2020). In contrast, the expansion of nanotechnology to plant sciences is relatively new
43 but has the capability to drastically improve conventional plant production systems.

44 Candidates for encapsulation and display that could be transported via nanoparticles in plants
45 include fertilizers, pesticides, fungicides, herbicides, biomolecules (such as DNA and proteins) and other
46 nutrients and growth enhancers. Currently, the use of these candidates directly (i.e., without
47 nanoparticle-based delivery) relies on oversaturation during application and a large portion is lost due to
48 runoff and degradation (Ladha *et al.*, 2005). For example, nitrogen fertilizer uptake efficiency by crops
49 after application is estimated to be 30-50% of that applied (Tilman *et al.*, 2002). Prospective
50 nanocarriers that lessen application waste by protecting the cargo, delivering it to a specific location,
51 and releasing the cargo in accordance with the demands of the plant could have a significant influence

52 on efficiency of use. The transient expression of bioactive molecules transported by ENPs into plant
53 systems will additionally allow for the incorporation of heterologous biological pathways and
54 development of “smart” crops that are more robust and productive. While the field of
55 phytonanotechnology is developing with the use of carriers such as single wall carbon nanotubes and
56 other abiotic nanoparticles, recent structural insights into Bacterial Microcompartments (BMCs),
57 proteinaceous organelles found in bacteria, suggest that the proteins of the BMC shell offer a promising
58 biotic building system for phytonanotechnology. While there are several efforts underway to transfer
59 the carboxysome, a BMC for CO₂ fixation, into plants (Price *et al.*, 2013; Zarzycki *et al.*, 2013; Atkinson *et*
60 *al.*, 2016; Hanson *et al.*, 2016; Long *et al.*, 2018), here we focus on the potential use of the shell proteins
61 common to all BMCs as a material for building nanocarriers for diverse applications in
62 phytonanotechnology.

63

64 **A Brief Summary of Characteristics of ENPs Currently Used in Phytonanotechnology**

65 Numerous ENPs are currently under development for phytonanotechnology (Wang *et al.*, 2016;
66 Jiang *et al.*, 2021; Agrawal *et al.*, 2022); these include liposomes (LPs) (Karny *et al.*, 2018), carbon
67 nanotubes (CNTs) (Serag *et al.*, 2011; Lahiani *et al.*, 2013; Kwak *et al.*, 2019; Demirer *et al.*, 2020),
68 mesoporous silica nanoparticles (MSNs) (Torney *et al.*, 2007; Martin-Ortigosa *et al.*, 2012; Chang *et al.*,
69 2013; Hussain *et al.*, 2013), gold nanoparticles (AuNPs) (Zhu *et al.*, 2012; Zhai *et al.*, 2014; Dan *et al.*,
70 2015), magnetic nanoparticles (MagNPs) (González-Melendi *et al.*, 2008; Huang *et al.*, 2011), metal
71 oxide nanoparticles (MONPs) (Kurepa *et al.*, 2010; Larue *et al.*, 2012; Rastogi *et al.*, 2017), and quantum
72 dots (QDs) (Etxeberria *et al.*, 2006; Koo *et al.*, 2015; Pang and Gong, 2019) (Table 1). Characterization of
73 each type of nanoparticle, particularly their capacity for bioactive compound transport, direct uptake by
74 plants, and toxicity to plants is of paramount importance. Certain ENPs are more applicable to specific
75 tasks in phytonanotechnology based on their overall structure. For instance, LPs, CNTs, MSNs (and

76 BMCs), which can encapsulate as well as display cargo, are more versatile in their utilization as
77 transporters while GNPs, MagNPs, MONPs, and QDs are relatively limited as they can only display cargo
78 on their surfaces. However, the smaller sized AuNPs, MagNPs, MONPs, and QDs can often more readily
79 translocate through subcellular barriers due to their minimal diameters. For example, the specific
80 localization of MagNPs within plant tissue was shown to be directly manipulatable through use of
81 magnetic gradients (González-Melendi *et al.*, 2008). The ability to encapsulate cargo is desired when
82 transporting degradable materials or when a sustained release of a substrate is desired. For instance, it
83 was reported that silica-based MSNs (ordered, honeycomb-like, porous nanoparticles), can be loaded
84 with the pesticide avermectin, protecting the substance from photodegradation and slowing its diffusion
85 into the surrounding microenvironment (Li *et al.*, 2007). MSNs have also been shown to be able to
86 encapsulate and transport the enzyme urease for hydrolysis of urea; a potential technique for the
87 controlled release of ammonia from urea fertilizer (Hossain *et al.*, 2008).

88 The use of ENPs for the delivery of plasmid DNA for genome incorporation or transient
89 expression is of particular interest as traditional methods are inefficient and tend to damage plant
90 tissue. Successful targeted delivery of plasmid DNA into plant tissues has been reported for several
91 ENPs, including CNTs, MSNs, AuNPs, and QDs (Etxeberria *et al.*, 2006; González-Melendi *et al.*, 2008; Wu
92 *et al.*, 2011; Martin-Ortigosa *et al.*, 2012). For example, CNTs, composed of cylinders of graphene, were
93 grafted with chitosan and shown to be able to capture plasmid DNA and passively translocate through
94 chloroplast membranes, with subsequent expression of the DNA within the chloroplast (Kwak *et al.*,
95 2019). Passive translocation was attributed to the high zeta potential on the exterior surface of the CNTs
96 and the overall diameter of the tubes (~20 nm). CNTs have also be reported to be able to penetrate
97 various subcellular membranes and target specific cellular substructures (Serag *et al.*, 2011).

98 Indeed, research to-date suggest that the interaction of ENPs with plant tissues and subcellular
99 structures depends on the physiochemical properties of the nanoparticle. Of particular importance in

100 these interactions are size, surface area, and surface electrostatic potential (Wong *et al.*, 2016). Entry of
101 ENPs into plants can occur via either aboveground tissues or organs (e.g., stigma, stomata, or leaf
102 surface wounds) or belowground root tissues (e.g., 'direct' uptake through root hairs or root surface
103 ruptures). To-date, only a few reports have detailed the 'direct' uptake and detection of ENPs into plants
104 (Zhu *et al.*, 2008, 2012; Corredor *et al.*, 2009; Serag *et al.*, 2011; Slomberg and Schoenfisch, 2012;
105 Hussain *et al.*, 2013; Zhai *et al.*, 2014; Dan *et al.*, 2015; Koo *et al.*, 2015; Wang *et al.*, 2016). Passive
106 'direct' uptake methods are appealing as they do not involve genetic modification of the plant, nor do
107 they immediately damage the plant. However, the majority of plant-nanocarrier studies have relied on
108 injection or particle bombardment for the incorporation of ENPs into plants or isolated plant cells or
109 organelles (Wang *et al.*, 2016). Although effective, these methods tend to damage plant tissues, are
110 labor intensive, and are impractical for widespread agricultural application of ENPs.

111 Once within plants, ENPs must overcome further translocation hurdles (Schwab *et al.*, 2016).
112 Barriers such as the stomata, the Casparian strip, the cell wall, and the cell membrane all have size-
113 exclusion thresholds for passage that must be met for uptake to occur. For instance, the cell wall of
114 plant cells limit translocation to particles with diameters ~20 nm (Wang *et al.*, 2016). ENPs with
115 diameters greater than 20 nm are likely to be blocked at this barrier. However, studies suggest a
116 flexibility to these size exclusion limits depending on the chemical microenvironment around the cell
117 wall and the specific physiochemical properties of the ENPs (Schwab *et al.*, 2016).

118 Beyond the cell wall, penetration of ENPs through the cell membrane has been demonstrated to
119 be particularly dependent on the electrostatic surface potential of the particle (Zhu *et al.*, 2012; Wong *et*
120 *al.*, 2016). The lipid exchange envelope penetration (LEEP) model surmises that the size and the zeta
121 potential of nanoparticles has the greatest influence on passive uptake through the cell membrane
122 (Wong *et al.*, 2016). A detailed report by Wong *et al.* (2016) reported that passive translocation of
123 different ENPs through the chloroplast membrane occurred for particles with diameters below 30 nm

124 and high magnitude surface zeta potentials (above 30 mV or below -30 mV). An increased understanding
125 of the requirements for efficient plant system transport to better traverse and overcome plant barriers
126 will allow for the development of more functional and transportable ENPs.

127 Although ENPs show promise to revolutionize food and agrochemical production, the relatively
128 new application of nanomaterials to the plant sciences necessitates considerable effort to assess
129 possible hazards that ENPs may pose (Kranjc and Drobne, 2019). Adverse environmental effects and the
130 capability for trophic transfer of toxic and stable ENPs in the food chain represent significant concerns
131 (Rodrigues *et al.*, 2017; Kranjc and Drobne, 2019). Research on the toxicity and impact of nanomaterials
132 on human/animal health have shown that adverse effects can result from exposure to certain ENPs.
133 (Pietrojusti *et al.*, 2018). Reports have detailed inflammation and scarring of the lungs due to inhalation
134 of multiwalled carbon nanotubes and carbon nanofibers, genotoxicity due to exposure to metal and
135 metal oxide nanoparticles, and have identified several ENPs as potential carcinogens (Fu *et al.*, 2014;
136 Kinaret *et al.*, 2017; Pietrojusti *et al.*, 2018). A wide range of factors, including plant species, application
137 route, duration of exposure, and the specific physicochemical properties and composition of the ENP
138 would all affect interactions with plants, toxicity, and transmissibility to the surrounding ecosystem (Ma
139 *et al.*, 2010; Nair *et al.*, 2010; Jiang *et al.*, 2021). These factors along with ENP adsorption, translocation,
140 localization, and bioaccumulation can contribute to both beneficial and adverse effects of the
141 nanoparticle on plant systems (Kranjc and Drobne, 2019). The future widespread application of
142 phytonanotechnology is dependent on the elimination of the toxic potential and a safe-by-design
143 approach should be the guiding principle for the development of all ENPs.

144

145 **Bacterial Microcompartment Shell Proteins: A New Building Block Set for**
146 **Phytonanotechnology**

147 A new candidate carrier for phytonanotechnology possessing the attributes that address many
148 of the concerns surrounding abiotic nanoparticles are Bacterial Microcompartment (BMC)-based
149 structures. BMCs have certain advantages that make them prime candidates for development within the
150 field of phytonanotechnology (Fig. 1). In nature, BMCs are functionally diverse, semi-permeable, self-
151 assembling protein organelles widely used by microorganisms to encapsulate biochemical pathways in
152 order to isolate reactive enzymes or toxic intermediates from the cytosol of the cell (Kerfeld *et al.*, 2018;
153 Sutter *et al.*, 2021). The basic architecture of the BMC membrane, the shell, is conserved across
154 different bacterial phyla but the reaction pathways they encapsulate are varied (Kerfeld *et al.*, 2018;
155 Sutter *et al.*, 2021). The most well studied BMC, the carboxysome, is found in all cyanobacteria and
156 some chemoautotrophs where it functions to sequester carbonic anhydrase and Ribulose-1,5-
157 bisphosphate carboxylase/oxygenase for CO₂ fixation (Kerfeld and Melnicki, 2016, 2016; Turmo *et al.*,
158 2017; Borden and Savage, 2021; Liu, 2022). Catabolic BMCs (also known as metabolosomes) include
159 those that are involved in the metabolism of organic compounds such as ethanolamine, propanediol,
160 fucose, and rhamnose (Bobik *et al.*, 1999; Kofoid *et al.*, 1999; Petit *et al.*, 2013; Erbilgin *et al.*, 2014). A
161 recent phylogenetic survey identified more than 7000 BMC loci including 68 types/subtypes of
162 metabolosomes, many of unknown function, highlighting their broad range of use by microorganisms
163 (Melnicki *et al.*, 2021; Sutter *et al.*, 2021).

164 The BMC shell is composed of three types of protein building blocks: a hexamer protein (BMC-
165 H), a trimer protein (BMC-T), and a pentamer protein (BMC-P) (Fig 2). The BMC-H component is the
166 most abundant type in shell formations and consists of six arranged monomers [Pfam00936 domain]
167 (Fig 2A). When assembled into a hexagonal oligomer, the BMC-H building block has a convex and
168 concave side with a thickness of ~20 Å and a diameter of ~70 Å (Kerfeld *et al.*, 2005). BMC-T proteins
169 consist of a tandem fusion of two Pfam00936 domains and the trimer resembles BMC-H hexamers
170 Because of this, BMC-T trimers are referred to as “pseudo-hexamers” (Klein *et al.*, 2009) (Fig 2A).

171 Additionally, there are two subtypes of the BMC-T proteins: a single trimer form and a second form
172 (BMC-T^{dp}) wherein two trimers dimerize across their concave faces (Klein *et al.*, 2009; Cai *et al.*, 2013). A
173 pore, located at the center of BMC-H, BMC-T, and BMC-T^{dp} oligomers serves as a selective-permeable
174 channel for metabolites (Kerfeld *et al.*, 2005; Klein *et al.*, 2009). At ~4-7 Å most pores are large enough
175 to permit the passage of small molecules such as bicarbonate and carboxylic acids but small enough to
176 exclude larger molecules. Pores of the BMC-T^{dp} trimer are larger at ~14 Å and are gated by absolutely
177 conserved residues (Klein *et al.*, 2009; Cai *et al.*, 2013; Larsson *et al.*, 2017; Mallette and Kimber, 2017).
178 The ability of BMC-T^{dp} proteins to dimerize across their concave surfaces results in an internal chamber
179 between the interior and exterior of the shell. In general, selective permeability of small molecules is
180 postulated to be determined by the polar residues lining the pore. This hypothesis is consistent with
181 studies that demonstrate alteration of BMC function when these residues are mutated (Chowdhury *et*
182 *al.*, 2015; Slininger Lee *et al.*, 2017). The BMC-P protein, which consists of a single monomer [Pfam03319
183 domain], forms a cyclical pentamer and serve to cap the vertices of the shell assemblies (Tanaka *et al.*,
184 2008; Sutter *et al.*, 2017). Shell formation without the BMC-P are possible and are referred to as “wiffle
185 ball” shells as they possess ~47 Å holes at the vertices where the BMC-P would be (Sutter, McGuire, *et*
186 *al.*, 2019; Kirst *et al.*, 2022) (Fig 2A). In addition to empty polyhedral shells, nanotube and sheet
187 architectures have been discovered through the heterologous overexpression of certain BMC hexamers
188 and BMC-T pseudohexamers; the sheets and nanotubes are composed of a single type of shell protein
189 (Fig. 2C & D) (Kerfeld and Erbilgin, 2015; Noël *et al.*, 2016; Uddin *et al.*, 2018). However, not all hexamer
190 and pseudohexamer BMC-T species can form nanotubes and sheets. The ability to form these structures
191 is likely dependent on the specific amino acid interactions on the edges of these hexamers which, as of
192 yet, have not been fully characterized. Once fully assembled, BMC shells have diameters ranging from 20
193 nm - 400 nm (depending on the BMC species type) and BMC-based nanotubes have diameters of 20 nm
194 (Parsons *et al.*, 2010; Lassila *et al.*, 2014; Sutter *et al.*, 2016; Sutter, McGuire, *et al.*, 2019).

195
196
197
198
199
200
201
202
203
204
205
206
207
208
209
210
211
212
213
214
215
216
217

Engineering Cargo Display and Encapsulation on BMC Shells

Although the main function of carboxysomes and metabosomes is the sequestration of enzymes and their reactive intermediates, a cardinal discovery of the last decade was that the formation of BMC shell membranes does not require cargo; empty shells can readily form (Parsons *et al.*, 2010; Lassila *et al.*, 2014; Sutter *et al.*, 2016; Hagen, Plegaria, *et al.*, 2018; Sutter, McGuire, *et al.*, 2019). Empty shells assembled without their corresponding cargo have been structurally characterized at atomic resolution with a combination of cryo-EM and x-ray crystallography, verifying their independent formation and structural stability (Sutter *et al.*, 2016, 2017; Sutter, Laughlin, *et al.*, 2019; Kalnins *et al.*, 2020). Moreover, these studies provided a structural blueprint of empty shells, detailing specific features like where the N- and C-termini of the shell proteins are positioned and the electrostatics of the interior and exterior. Detailed knowledge of the structural characteristics of these assemblies is foundational not only for understanding the role of the shell in native BMC function but additionally enables for the precise bioengineering of shell components and positioning of cargo to exterior and luminal surfaces. In these studies, the N- and C-termini of the shell proteins were shown to be located on the external surface of the assemblies. This informed designs for displaying proteins on the outside facets of shells and nanotubes (Kalnins *et al.*, 2020). Using both termini of a hexamer allows for the potential fusion of two distinct elements (one attached at each terminus) per monomer; for a total of twelve attachments points. The ability to display enzymatic cargo on the exterior of these architectures is beneficial, for example, to catalyze a reaction to accumulate a substantial concentration of substrate adjacent to the central protein pores for rapid diffusion to the interior. Likewise, identification of interior surface residues permits the swapping of sidechains for tailored interaction with cargo through electrostatic association. Ensuing development of circularly permuted hexamers that display the termini

218 on the luminal surface of a shell enabled encapsulation of fused cargo to the interior (Ferlez *et al.*,
219 2019).

220 Initial attempts at heterologous cargo loading of BMC shells utilized encapsulation peptides that
221 are present in many BMCs, however, studies using this method reported meager loading efficiency
222 (Lassila *et al.*, 2014; Aussignargues *et al.*, 2015; Wagner *et al.*, 2017; Hagen, Sutter, *et al.*, 2018). Since
223 then, further progress has been made to modify the structural proteins to display and encapsulate
224 cargo. Using the SpyTag/SpyCatcher split bacterial adhesion system (Veggiani *et al.*, 2016), the
225 shortcomings of the encapsulation peptide strategy were circumvented and a new method was
226 developed for encapsulation (Hagen, Sutter, *et al.*, 2018). This method relies on the formation of a
227 covalent bond when the independent domains of the SpyTag and SpyCatcher interact. By modifying a
228 region on the luminal side of the BMC-T component to include a loop containing the 1.4 kDa SpyTag
229 element, encapsulation of heterologous cargo containing the 9 kDa SpyCatcher element to the interior
230 surface was made possible. Loading and attachment of cargo via this adhesion system is possible *in vivo*
231 through recombinant expression of the shell proteins along with expression of cargo proteins and *in*
232 *vitro* via diffusion of cargo through the gaps of wiffle ball shells with subsequent pentamer “capping” to
233 create fully encapsulated shells. Moreover, the “capping” strategy using pentamers that are
234 functionalized with an affinity tag allows for purification of the full formed and loaded shells (Hagen,
235 Plegaria, *et al.*, 2018).

236 Thus far, several model shell system platforms have been developed and include the PDU
237 (propanediol utilization) BMC shells and HO (*Haliangium ochraceum*) BMC shells (Parsons *et al.*, 2008;
238 Lassila *et al.*, 2014). Utilizing these and other BMC shell membranes, several synthetic nanoreactors
239 have been constructed that include a PDU encapsulating ethanol bioreactor that is able to transform
240 pyruvate to ethanol (Lawrence *et al.*, 2014), a *Citrobacter freundii* bacterial microcompartment-based
241 system that can accumulate and store polyphosphate (Liang *et al.*, 2017), and a hydrogen-producing α -

242 carboxysome shell nanoreactor (Li *et al.*, 2020). Recently, employing the HO shell platform, a synthetic
243 formate utilizing BMC was developed that encapsulated two distinct enzymes, the oxygen-sensitive
244 glycol radical enzyme pyruvate formate lyase and a phosphate acyltransferase (Kirst *et al.*, 2022). In this
245 study, researchers were able to take advantage of the SpyTag/SpyCatcher system to attach one enzyme
246 and the second was incorporated with the similarly functioning SnoopTag/SnoopCatcher split adhesion
247 system. In another recent report that highlights the modifiability of BMC shell components, a synthetic
248 hexagonal trimer protein was engineered through the tandem fusion of two domains of the BMC-H,
249 creating cyclic trimers (designated BMC-H²) that self-assemble to form icosahedral wiffle ball shells with
250 gaps at the pentamer positions (Sutter, McGuire, *et al.*, 2019). The generated BMC-H² shell had a smaller
251 diameter (25 nm) than the typical BMC-H-containing minimal shell (40 nm). This method of shell protein
252 engineering opens the possibility of fusing two distinct hexamer domains together from disparate
253 species to create unique cyclic trimer proteins containing two different sets of residues on their surfaces
254 and on the periphery of the central pore; as compared to the repeated residues for typical
255 homohexameric proteins.

256 In regard to the other BMC-based architectures, numerous different species of hexamers have
257 been identified that can readily form nanotube and sheet structures but more research is needed to
258 elucidate and take advantage of the subtle differences that dictate the differences in the resulting self-
259 assembled morphologies (Parsons *et al.*, 2010; Lassila *et al.*, 2014; Pang *et al.*, 2014; Cai *et al.*, 2016;
260 Noël *et al.*, 2016; Sutter *et al.*, 2016; Uddin *et al.*, 2018) (Fig. 3). Nanotube and sheet architectures have
261 several distinct features relative to shells. For example, nanotubes are formed by a single type of protein
262 (Parsons *et al.*, 2010; Noël *et al.*, 2016). While the diameter of nanotubes is in the range of that of shell
263 structures (~20 nm), they can be micrometers in length (Fig. 3C, D) (Noël *et al.*, 2016). Likewise, BMC-
264 based protein sheets are also composed of a single protein and can have planar dimensions that range
265 in size up to micrometers (Fig. 3E, F) (Sutter *et al.*, 2016). Both sheets and tubes could serve as binding

266 surfaces to organize, immobilize, and pack closely together, large quantities of enzymes or other
267 bioactive molecules or could additionally serve as structure-enhancing elements to modify the stability
268 of plant cells. Given that these structures are composed of a single BMC element, their assembly is much
269 simpler, and their formation doesn't depend on stoichiometric ratios of several different shell
270 components as is the case for BMC-based shells. These structures are also highly modifiable. Slight
271 deviations in how the hexamers of these architectures interact along their edges could, for example,
272 result in nanotubes of varying diameters and rigidity or sheets with slight curvatures or repeating
273 undulations across their surfaces that could be taken advantage of for bioengineering purposes.

274

275 **Advantages of BMC Architectures for Phytonanotechnology**

276 The recent advances in functionalizing BMC-based shell components demonstrate the future
277 potential for use of BMC-based architectures as nanocarriers or scaffolds. The architectures being
278 developed offer a wide range of applicability for phytonanotechnology. Because BMC-based
279 architectures are composed entirely of protein, these structures are biodegradable, can be rapidly
280 produced and modified for functionality *in vitro* (Fig. 1A), and are able to be expressed directly *in vivo*
281 within the plants through transient expression or genome incorporation (Fig. 1B). Unlike carbon-, metal-
282 , or lipid-based ENPs that are not genetically encoded, BMCs can readily be fine-tuned to “program”
283 charge, hydrophobicity, surface structure, etc., through codon mutagenesis. *In vitro* assembly reactions
284 for BMC-based architectures are typically conducted in neutral or slightly alkaline buffer solutions
285 (Hagen, Plegaria, *et al.*, 2018), which is similar to the internal environment of plant cells that, under
286 normal condition, have a cytosolic pH of 7.5 (Kader and Lindberg, 2010). The stability of these
287 architectures in distinct plant cell compartments that possess more acidic pH environments is less
288 certain, however, and their use in such compartments would need to be further investigated to
289 elucidate the viability of their use there. Both synthetic BMC shells and nanotubes possess diameters

290 that meet or are close to the size exclusion limit requirements (~20 nm) of plant transport barriers.
291 Because they are genetically encoded, it is relatively trivial to modify surface residues of BMC-based
292 shells and nanotubes to tune the zeta potential, which has been shown to be important for passive
293 membrane translocation via the LEEP mechanism (Fig. 3B & D) (Wong *et al.*, 2016). However, as of yet,
294 the ability of translocation of BMC-based shells or nanotubes to translocate through membranes or
295 between plant cell compartments via this mechanism has not been experimentally confirmed.

296 The functional diversity of catabolic BMCs found in nature underscores the adaptability of the
297 BMC shell system for various biochemical pathways (Melnicki *et al.*, 2021; Sutter *et al.*, 2021).
298 Bioinformatic analyses along with structural characterizations of BMC shell systems have demonstrated
299 shared universal principles of shell building blocks that can be taken advantage of for the engineering of
300 mix-and-match, function-specific structures (Sutter *et al.*, 2017, 2021). When further developed, this
301 catalog of interchangeable building blocks provides an inventory of components to select from for
302 precise engineering BMC architectures for phytonanotechnology. Engineering of the central pore
303 present in the hexamer, trimers, and pseudohexamers can be explored to allow for selective uptake of
304 substrates including electrons; metal centers have been introduced into pores (Aussignargues *et al.*,
305 2016; Plegaria *et al.*, 2020). Likewise, the pores may be of use for the controlled release of encapsulated
306 substances. The redesign of pores could grant the controlled-uptake of nutrients and substrates to
307 interact with encapsulated enzymes or the controlled-release of fertilizers, pesticides, or other
308 agrochemicals that can interact directly to benefit the plant.

309

310 **Future Prospects and Concluding Remarks**

311 The development of green nanotechnology platforms, such as protein-based BMC architectures,
312 and their application in the field of phytonanotechnology show immense potential. BMC-based shells,
313 nanotubes, and sheets are promising for research in this field due to their ease of production,

314 multifunctionality, and biodegradability, however, the interactions between BMC structures and plant
315 systems are yet to be explored. Studies that focus on these interactions will help to guide future
316 development of BMC-based platforms in this field. Several methods are currently available for cargo
317 loading onto BMCs but novel methods that permit the controlled, targeted release of cargo are
318 necessary for the development of “smart” systems of transport. Incorporation of agriculture-relevant
319 agrochemicals and biomolecules during future attachment experimentation will be important to assess
320 feasibility in phytonanotechnology.

321 The expression of BMC-based architectures in plants is yet another interesting possible avenue
322 for application of these platforms. Expression of nanotubes or sheets could potentially affect the rigidity
323 and structural stability of plant cells or could serve as unique scaffolds for the attachment of enzymes,
324 agrochemicals, or bioactive molecules. As with all ENPs, rigorous studies to elucidate possible plant
325 toxicity and ecotoxicity related to direct uptake and expression of BMCs within plant systems must be
326 conducted to ensure safe use and to establish social acceptance of the technology.

327

328 **Acknowledgements**

329 This work was supported by the Office of Science of the US Department of Energy DE-FG02-91ER20021
330 and MSU AgBio Research.

331 The authors would like to thank Lior Doron and Matthew Dwyer for helpful comments on the
332 manuscript. Markus Sutter, Sigal Lechno-Yossef, Roberto Espinoza Corral, Liwei Hui, Eric Young, and
333 Damien Sheppard for their comments and suggestions on the figures, and Henning Kirst for providing
334 Figures 3B and 3F.

335 **References**

- 336 Agrawal, S., Kumar, V., Kumar, S., and Shahi, S.K. (2022) Plant development and crop protection using
 337 phytonanotechnology: A new window for sustainable agriculture. *Chemosphere* **299**: 134465.
- 338 Atkinson, N., Feike, D., Mackinder, L.C.M., Meyer, M.T., Griffiths, H., Jonikas, M.C., et al. (2016)
 339 Introducing an algal carbon-concentrating mechanism into higher plants: location and
 340 incorporation of key components. *Plant Biotechnol J* **14**: 1302–1315.
- 341 Aussignargues, C., Paasch, B.C., Gonzalez-Esquer, R., Erbilgin, O., and Kerfeld, C.A. (2015) Bacterial
 342 microcompartment assembly: The key role of encapsulation peptides. *Commun Integr Biol* **8**:
 343 e1039755.
- 344 Aussignargues, C., Pandelia, M.-E., Sutter, M., Plegaria, J.S., Zarzycki, J., Turmo, A., et al. (2016) Structure
 345 and Function of a Bacterial Microcompartment Shell Protein Engineered to Bind a [4Fe-4S]
 346 Cluster. *J Am Chem Soc* **138**: 5262–5270.
- 347 Bobik, T.A., Havemann, G.D., Busch, R.J., Williams, D.S., and Aldrich, H.C. (1999) The propanediol
 348 utilization (pdu) operon of *Salmonella enterica* serovar Typhimurium LT2 includes genes
 349 necessary for formation of polyhedral organelles involved in coenzyme B(12)-dependent 1, 2-
 350 propanediol degradation. *J Bacteriol* **181**: 5967–5975.
- 351 Borden, J.S. and Savage, D.F. (2021) New discoveries expand possibilities for carboxysome engineering.
 352 *Curr Opin Microbiol* **61**: 58–66.
- 353 Cai, F., Bernstein, S.L., Wilson, S.C., and Kerfeld, C.A. (2016) Production and Characterization of Synthetic
 354 Carboxysome Shells with Incorporated Luminal Proteins. *Plant Physiol* **170**: 1868–1877.
- 355 Cai, F., Sutter, M., Cameron, J.C., Stanley, D.N., Kinney, J.N., and Kerfeld, C.A. (2013) The structure of
 356 CcmP, a tandem bacterial microcompartment domain protein from the β -carboxysome, forms a
 357 subcompartment within a microcompartment. *J Biol Chem* **288**: 16055–16063.
- 358 Chang, F.-P., Kuang, L.-Y., Huang, C.-A., Jane, W.-N., Hung, Y., Hsing, Y.C., and Mou, C.-Y. (2013) A simple
 359 plant gene delivery system using mesoporous silica nanoparticles as carriers. *J Mater Chem B* **1**:
 360 5279–5287.
- 361 Chowdhury, C., Chun, S., Pang, A., Sawaya, M.R., Sinha, S., Yeates, T.O., and Bobik, T.A. (2015) Selective
 362 molecular transport through the protein shell of a bacterial microcompartment organelle. *PNAS*
 363 **112**: 2990–2995.
- 364 Corredor, E., Testillano, P.S., Coronado, M.-J., González-Melendi, P., Fernández-Pacheco, R., Marquina,
 365 C., et al. (2009) Nanoparticle penetration and transport in living pumpkin plants: in
 366 situsubcellular identification. *BMC Plant Biology* **9**: 45.
- 367 Cunningham, F.J., Goh, N.S., Demirer, G.S., Matos, J.L., and Landry, M.P. (2018) Nanoparticle-Mediated
 368 Delivery towards Advancing Plant Genetic Engineering. *Trends in Biotechnology* **36**: 882–897.
- 369 Dan, Y., Zhang, W., Xue, R., Ma, X., Stephan, C., and Shi, H. (2015) Characterization of Gold Nanoparticle
 370 Uptake by Tomato Plants Using Enzymatic Extraction Followed by Single-Particle Inductively
 371 Coupled Plasma–Mass Spectrometry Analysis. *Environ Sci Technol* **49**: 3007–3014.
- 372 Demirer, G.S., Zhang, H., Goh, N.S., Pinals, R.L., Chang, R., and Landry, M.P. (2020) Carbon nanocarriers
 373 deliver siRNA to intact plant cells for efficient gene knockdown. *Science Advances* **6**: eaaz0495.
- 374 Demirer, G.S., Zhang, H., Matos, J.L., Goh, N.S., Cunningham, F.J., Sung, Y., et al. (2019) High aspect ratio
 375 nanomaterials enable delivery of functional genetic material without DNA integration in mature
 376 plants. *Nat Nanotechnol* **14**: 456–464.
- 377 Erbilgin, O., McDonald, K.L., and Kerfeld, C.A. (2014) Characterization of a Planctomycetal Organelle: A
 378 Novel Bacterial Microcompartment for the Aerobic Degradation of Plant Saccharides. *Applied
 379 and Environmental Microbiology*.

- 380 Etxeberria, E., Gonzalez, P., Baroja-Fernández, E., and Romero, J.P. (2006) Fluid Phase Endocytic Uptake
381 of Artificial Nano-Spheres and Fluorescent Quantum Dots by Sycamore Cultured Cells. *Plant*
382 *Signaling & Behavior* **1**: 196–200.
- 383 Ferlez, B., Sutter, M., and Kerfeld, C.A. (2019) A Designed Bacterial Microcompartment Shell with
384 Tunable Composition and Precision Cargo Loading. *Metab Eng* **54**: 286–291.
- 385 Fu, P.P., Xia, Q., Hwang, H.-M., Ray, P.C., and Yu, H. (2014) Mechanisms of nanotoxicity: generation of
386 reactive oxygen species. *J Food Drug Anal* **22**: 64–75.
- 387 González-Melendi, P., Fernández-Pacheco, R., Coronado, M.J., Corredor, E., Testillano, P.S., Risueño,
388 M.C., et al. (2008) Nanoparticles as Smart Treatment-delivery Systems in Plants: Assessment of
389 Different Techniques of Microscopy for their Visualization in Plant Tissues. *Annals of Botany* **101**:
390 187–195.
- 391 Hagen, A., Plegaria, J.S., Sloan, N., Ferlez, B., Aussignargues, C., Burton, R., and Kerfeld, C.A. (2018) In
392 Vitro Assembly of Diverse Bacterial Microcompartment Shell Architectures. *Nano Lett* **18**: 7030–
393 7037.
- 394 Hagen, A., Sutter, M., Sloan, N., and Kerfeld, C.A. (2018) Programmed loading and rapid purification of
395 engineered bacterial microcompartment shells. *Nat Commun* **9**: 2881.
- 396 Hanson, M.R., Lin, M.T., Carmo-Silva, A.E., and Parry, M.A.J. (2016) Towards engineering carboxysomes
397 into C3 plants. *Plant J* **87**: 38–50.
- 398 Hatami, M., Kariman, K., and Ghorbanpour, M. (2016) Engineered nanomaterial-mediated changes in
399 the metabolism of terrestrial plants. *Sci Total Environ* **571**: 275–291.
- 400 Hossain, K.-Z., Monreal, C.M., and Sayari, A. (2008) Adsorption of urease on PE-MCM-41 and its catalytic
401 effect on hydrolysis of urea. *Colloids Surf B Biointerfaces* **62**: 42–50.
- 402 Huang, X., Stein, B.D., Cheng, H., Malyutin, A., Tsvetkova, I.B., Baxter, D.V., et al. (2011) Magnetic Virus-
403 like Nanoparticles in *N. benthamiana* Plants: A New Paradigm for Environmental and Agronomic
404 Biotechnological Research. *ACS Nano* **5**: 4037–4045.
- 405 Hussain, H.I., Yi, Z., Rookes, J.E., Kong, L.X., and Cahill, D.M. (2013) Mesoporous silica nanoparticles as a
406 biomolecule delivery vehicle in plants. *J Nanopart Res* **15**: 1676.
- 407 Jiang, M., Song, Y., Kanwar, M.K., Ahammed, G.J., Shao, S., and Zhou, J. (2021) Phytonanotechnology
408 applications in modern agriculture. *Journal of Nanobiotechnology* **19**: 430.
- 409 Kader, M.A. and Lindberg, S. (2010) Cytosolic calcium and pH signaling in plants under salinity stress.
410 *Plant Signal Behav* **5**: 233–238.
- 411 Kalnins, G., Cesle, E.-E., Jansons, J., Liepins, J., Filimonenko, A., and Tars, K. (2020) Encapsulation
412 mechanisms and structural studies of GRM2 bacterial microcompartment particles. *Nat*
413 *Commun* **11**: 388.
- 414 Karny, A., Zinger, A., Kajal, A., Shainsky-Roitman, J., and Schroeder, A. (2018) Therapeutic nanoparticles
415 penetrate leaves and deliver nutrients to agricultural crops. *Sci Rep* **8**: 7589.
- 416 Kerfeld, C.A., Aussignargues, C., Zarzycki, J., Cai, F., and Sutter, M. (2018) Bacterial microcompartments.
417 *Nat Rev Microbiol* **16**: 277–290.
- 418 Kerfeld, C.A. and Erbilgin, O. (2015) Bacterial microcompartments and the modular construction of
419 microbial metabolism. *Trends in Microbiology* **23**: 22–34.
- 420 Kerfeld, C.A. and Melnicki, M.R. (2016) Assembly, function and evolution of cyanobacterial
421 carboxysomes. *Curr Opin Plant Biol* **31**: 66–75.
- 422 Kerfeld, C.A., Sawaya, M.R., Tanaka, S., Nguyen, C.V., Phillips, M., Beeby, M., and Yeates, T.O. (2005)
423 Protein structures forming the shell of primitive bacterial organelles. *Science* **309**: 936–938.
- 424 Kinaret, P., Ilves, M., Fortino, V., Rydman, E., Karisola, P., Lähde, A., et al. (2017) Inhalation and
425 Oropharyngeal Aspiration Exposure to Rod-Like Carbon Nanotubes Induce Similar Airway
426 Inflammation and Biological Responses in Mouse Lungs. *ACS Nano* **11**: 291–303.

- 427 Kirst, H., Ferlez, B.H., Lindner, S.N., Cotton, C.A.R., Bar-Even, A., and Kerfeld, C.A. (2022) Toward a glycol
428 radical enzyme containing synthetic bacterial microcompartment to produce pyruvate from
429 formate and acetate. *Proceedings of the National Academy of Sciences* **119**: e2116871119.
- 430 Klein, M.G., Zwart, P., Bagby, S.C., Cai, F., Chisholm, S.W., Heinhorst, S., et al. (2009) Identification and
431 structural analysis of a novel carboxysome shell protein with implications for metabolite
432 transport. *J Mol Biol* **392**: 319–333.
- 433 Kofoid, E., Rappleye, C., Stojiljkovic, I., and Roth, J. (1999) The 17-gene ethanolamine (eut) operon of
434 *Salmonella typhimurium* encodes five homologues of carboxysome shell proteins. *J Bacteriol*
435 **181**: 5317–5329.
- 436 Koo, Y., Wang, J., Zhang, Q., Zhu, H., Chehab, E.W., Colvin, V.L., et al. (2015) Fluorescence Reports Intact
437 Quantum Dot Uptake into Roots and Translocation to Leaves of *Arabidopsis thaliana* and
438 Subsequent Ingestion by Insect Herbivores. *Environ Sci Technol* **49**: 626–632.
- 439 Kranjc, E. and Drobne, D. (2019) Nanomaterials in Plants: A Review of Hazard and Applications in the
440 Agri-Food Sector. *Nanomaterials (Basel)* **9**: E1094.
- 441 Kurepa, J., Paunesku, T., Vogt, S., Arora, H., Rabatic, B.M., Lu, J., et al. (2010) Uptake and Distribution of
442 Ultrasmall Anatase TiO₂ Alizarin Red S Nanoconjugates in *Arabidopsis thaliana*. *Nano Lett* **10**:
443 2296–2302.
- 444 Kwak, S.-Y., Lew, T.T.S., Sweeney, C.J., Koman, V.B., Wong, M.H., Bohmert-Tatarev, K., et al. (2019)
445 Chloroplast-selective gene delivery and expression in planta using chitosan-complexed single-
446 walled carbon nanotube carriers. *Nat Nanotechnol* **14**: 447–455.
- 447 Ladha, J.K., Pathak, H., J. Krupnik, T., Six, J., and van Kessel, C. (2005) Efficiency of Fertilizer Nitrogen in
448 Cereal Production: Retrospects and Prospects. In *Advances in Agronomy*. Academic Press, pp.
449 85–156.
- 450 Lahiani, M.H., Dervishi, E., Chen, J., Nima, Z., Gaume, A., Biris, A.S., and Khodakovskaya, M.V. (2013)
451 Impact of Carbon Nanotube Exposure to Seeds of Valuable Crops. *ACS Appl Mater Interfaces* **5**:
452 7965–7973.
- 453 Larsson, A.M., Hasse, D., Valegård, K., and Andersson, I. (2017) Crystal structures of β -carboxysome shell
454 protein CcmP: ligand binding correlates with the closed or open central pore. *J Exp Bot* **68**:
455 3857–3867.
- 456 Larue, C., Laurette, J., Herlin-Boime, N., Khodja, H., Fayard, B., Flank, A.-M., et al. (2012) Accumulation,
457 translocation and impact of TiO₂ nanoparticles in wheat (*Triticum aestivum* spp.): Influence of
458 diameter and crystal phase. *Science of The Total Environment* **431**: 197–208.
- 459 Lassila, J.K., Bernstein, S.L., Kinney, J.N., Axen, S.D., and Kerfeld, C.A. (2014) Assembly of robust bacterial
460 microcompartment shells using building blocks from an organelle of unknown function. *J Mol*
461 *Biol* **426**: 2217–2228.
- 462 Lawrence, A.D., Frank, S., Newnham, S., Lee, M.J., Brown, I.R., Xue, W.-F., et al. (2014) Solution structure
463 of a bacterial microcompartment targeting peptide and its application in the construction of an
464 ethanol bioreactor. *ACS Synth Biol* **3**: 454–465.
- 465 Li, T., Jiang, Q., Huang, J., Aitchison, C.M., Huang, F., Yang, M., et al. (2020) Reprogramming bacterial
466 protein organelles as a nanoreactor for hydrogen production. *Nat Commun* **11**: 5448.
- 467 Li, Z.-Z., Chen, J.-F., Liu, F., Liu, A.-Q., Wang, Q., Sun, H.-Y., and Wen, L.-X. (2007) Study of UV-shielding
468 properties of novel porous hollow silica nanoparticle carriers for avermectin. *Pest Management*
469 *Science* **63**: 241–246.
- 470 Liang, M., Frank, S., Lünsdorf, H., Warren, M.J., and Prentice, M.B. (2017) Bacterial microcompartment-
471 directed polyphosphate kinase promotes stable polyphosphate accumulation in *E. coli*.
472 *Biotechnol J* **12**.
- 473 Liu, L.-N. (2022) Advances in the bacterial organelles for CO₂ fixation. *Trends Microbiol* **30**: 567–580.

- 474 Long, B.M., Hee, W.Y., Sharwood, R.E., Rae, B.D., Kaines, S., Lim, Y.-L., et al. (2018) Carboxysome
475 encapsulation of the CO₂-fixing enzyme Rubisco in tobacco chloroplasts. *Nat Commun* **9**: 3570.
- 476 Ma, X., Geiser-Lee, J., Deng, Y., and Kolmakov, A. (2010) Interactions between engineered nanoparticles
477 (ENPs) and plants: Phytotoxicity, uptake and accumulation. *Science of The Total Environment*
478 **408**: 3053–3061.
- 479 Mallette, E. and Kimber, M.S. (2017) A Complete Structural Inventory of the Mycobacterial
480 Microcompartment Shell Proteins Constrains Models of Global Architecture and Transport.
481 *Journal of Biological Chemistry* **292**: 1197–1210.
- 482 Martin-Ortigosa, S., Valenstein, J.S., Sun, W., Moeller, L., Fang, N., Trewyn, B.G., et al. (2012) Parameters
483 affecting the efficient delivery of mesoporous silica nanoparticle materials and gold nanorods
484 into plant tissues by the biolistic method. *Small* **8**: 413–422.
- 485 Melnicki, M.R., Sutter, M., and Kerfeld, C.A. (2021) Evolutionary relationships among shell proteins of
486 carboxysomes and metabolosomes. *Current Opinion in Microbiology* **63**: 1–9.
- 487 Nair, R., Varghese, S.H., Nair, B.G., Maekawa, T., Yoshida, Y., and Kumar, D.S. (2010) Nanoparticulate
488 material delivery to plants. *Plant Science* **179**: 154–163.
- 489 Neupane, G.P., Ma, W., Yildirim, T., Tang, Y., Zhang, L., and Lu, Y. (2019) 2D organic semiconductors, the
490 future of green nanotechnology. *Nano Materials Science* **1**: 246–259.
- 491 Noël, C.R., Cai, F., and Kerfeld, C.A. (2016) Purification and Characterization of Protein Nanotubes
492 Assembled from a Single Bacterial Microcompartment Shell Subunit. *Advanced Materials*
493 *Interfaces* **3**: 1500295.
- 494 Pang, A., Frank, S., Brown, I., Warren, M.J., and Pickersgill, R.W. (2014) Structural insights into higher
495 order assembly and function of the bacterial microcompartment protein PduA. *J Biol Chem* **289**:
496 22377–22384.
- 497 Pang, C. and Gong, Y. (2019) Current Status and Future Prospects of Semiconductor Quantum Dots in
498 Botany. *J Agric Food Chem* **67**: 7561–7568.
- 499 Parsons, J.B., Dinesh, S.D., Deery, E., Leech, H.K., Brindley, A.A., Heldt, D., et al. (2008) Biochemical and
500 Structural Insights into Bacterial Organelle Form and Biogenesis. *Journal of Biological Chemistry*
501 **283**: 14366–14375.
- 502 Parsons, J.B., Frank, S., Bhella, D., Liang, M., Prentice, M.B., Mulvihill, D.P., and Warren, M.J. (2010)
503 Synthesis of Empty Bacterial Microcompartments, Directed Organelle Protein Incorporation, and
504 Evidence of Filament-Associated Organelle Movement. *Molecular Cell* **38**: 305–315.
- 505 Petit, E., LaTouf, W.G., Coppi, M.V., Warnick, T.A., Currie, D., Romashko, I., et al. (2013) Involvement of a
506 Bacterial Microcompartment in the Metabolism of Fucose and Rhamnose by Clostridium
507 phytofermentans. *PLOS ONE* **8**: e54337.
- 508 Pietroiusti, A., Stockmann-Juvala, H., Lucaroni, F., and Savolainen, K. (2018) Nanomaterial exposure,
509 toxicity, and impact on human health. *Wiley Interdiscip Rev Nanomed Nanobiotechnol* **10**:
510 e1513.
- 511 Plegaria, J.S., Yates, M.D., Glaven, S.M., and Kerfeld, C.A. (2020) Redox Characterization of Electrode-
512 Immobilized Bacterial Microcompartment Shell Proteins Engineered to Bind Metal Centers. *ACS*
513 *Appl Bio Mater* **3**: 685–692.
- 514 Price, G.D., Pengelly, J.J.L., Forster, B., Du, J., Whitney, S.M., von Caemmerer, S., et al. (2013) The
515 cyanobacterial CCM as a source of genes for improving photosynthetic CO₂ fixation in crop
516 species. *J Exp Bot* **64**: 753–768.
- 517 Rastogi, A., Zivcak, M., Sytar, O., Kalaji, H.M., He, X., Mbarki, S., and Brestic, M. (2017) Impact of Metal
518 and Metal Oxide Nanoparticles on Plant: A Critical Review. *Front Chem* **5**: 78.
- 519 Rodrigues, S.M., Demokritou, P., Dokoozlian, N., Hendren, C.O., Karn, B., Mauter, M.S., et al. (2017)
520 Nanotechnology for sustainable food production: promising opportunities and scientific
521 challenges. *Environ Sci: Nano* **4**: 767–781.

- 522 Schwab, F., Zhai, G., Kern, M., Turner, A., Schnoor, J.L., and Wiesner, M.R. (2016) Barriers, pathways and
 523 processes for uptake, translocation and accumulation of nanomaterials in plants – Critical
 524 review. *Nanotoxicology* **10**: 257–278.
- 525 Serag, M.F., Kaji, N., Gaillard, C., Okamoto, Y., Terasaka, K., Jabasini, M., et al. (2011) Trafficking and
 526 Subcellular Localization of Multiwalled Carbon Nanotubes in Plant Cells. *ACS Nano* **5**: 493–499.
- 527 Shang, Y., Hasan, M.K., Ahammed, G.J., Li, M., Yin, H., and Zhou, J. (2019) Applications of
 528 Nanotechnology in Plant Growth and Crop Protection: A Review. *Molecules* **24**: E2558.
- 529 Slininger Lee, M.F., Jakobson, C.M., and Tullman-Ercek, D. (2017) Evidence for Improved Encapsulated
 530 Pathway Behavior in a Bacterial Microcompartment through Shell Protein Engineering. *ACS*
 531 *Synth Biol* **6**: 1880–1891.
- 532 Slomberg, D.L. and Schoenfisch, M.H. (2012) Silica Nanoparticle Phytotoxicity to *Arabidopsis thaliana*.
 533 *Environ Sci Technol* **46**: 10247–10254.
- 534 Smith, D.M., Simon, J.K., and Baker Jr, J.R. (2013) Applications of nanotechnology for immunology. *Nat*
 535 *Rev Immunol* **13**: 592–605.
- 536 Sutter, M., Faulkner, M., Aussignargues, C., Paasch, B.C., Barrett, S., Kerfeld, C.A., and Liu, L.-N. (2016)
 537 Visualization of Bacterial Microcompartment Facet Assembly Using High-Speed Atomic Force
 538 Microscopy. *Nano Lett* **16**: 1590–1595.
- 539 Sutter, M., Greber, B., Aussignargues, C., and Kerfeld, C.A. (2017) Assembly principles and structure of a
 540 6.5-MDa bacterial microcompartment shell. *Science* **356**: 1293–1297.
- 541 Sutter, M., Laughlin, T.G., Sloan, N.B., Serwas, D., Davies, K.M., and Kerfeld, C.A. (2019) Structure of a
 542 Synthetic β -Carboxysome Shell. *Plant Physiology* **181**: 1050–1058.
- 543 Sutter, M., McGuire, S., Ferlez, B., and Kerfeld, C.A. (2019) Structural Characterization of a Synthetic
 544 Tandem-Domain Bacterial Microcompartment Shell Protein Capable of Forming Icosahedral
 545 Shell Assemblies. *ACS Synth Biol* **8**: 668–674.
- 546 Sutter, M., Melnicki, M.R., Schulz, F., Woyke, T., and Kerfeld, C.A. (2021) A catalog of the diversity and
 547 ubiquity of bacterial microcompartments. *Nat Commun* **12**: 3809.
- 548 Tanaka, S., Kerfeld, C.A., Sawaya, M.R., Cai, F., Heinhorst, S., Cannon, G.C., and Yeates, T.O. (2008)
 549 Atomic-Level Models of the Bacterial Carboxysome Shell. *Science* **319**: 1083–1086.
- 550 Tilman, D., Cassman, K.G., Matson, P.A., Naylor, R., and Polasky, S. (2002) Agricultural sustainability and
 551 intensive production practices. *Nature* **418**: 671–677.
- 552 Torney, F., Trewyn, B.G., Lin, V.S.-Y., and Wang, K. (2007) Mesoporous silica nanoparticles deliver DNA
 553 and chemicals into plants. *Nature Nanotech* **2**: 295–300.
- 554 Turmo, A., Gonzalez-Esquer, C.R., and Kerfeld, C.A. (2017) Carboxysomes: metabolic modules for CO₂
 555 fixation. *FEMS Microbiol Lett* **364**.
- 556 Uddin, I., Frank, S., Warren, M.J., and Pickersgill, R.W. (2018) A Generic Self-Assembly Process in
 557 Microcompartments and Synthetic Protein Nanotubes. *Small* **14**: e1704020.
- 558 Vega-Vásquez, P., Mosier, N.S., and Irudayaraj, J. (2020) Nanoscale Drug Delivery Systems: From
 559 Medicine to Agriculture. *Front Bioeng Biotechnol* **8**: 79.
- 560 Veggiani, G., Nakamura, T., Brenner, M.D., Gayet, R.V., Yan, J., Robinson, C.V., and Howarth, M. (2016)
 561 Programmable polyproteins built using twin peptide superglues. *Proceedings of the National*
 562 *Academy of Sciences* **113**: 1202–1207.
- 563 Wagner, H.J., Capitain, C.C., Richter, K., Nessling, M., and Mampel, J. (2017) Engineering bacterial
 564 microcompartments with heterologous enzyme cargos. *Engineering in Life Sciences* **17**: 36–46.
- 565 Wang, P., Lombi, E., Zhao, F.-J., and Kopittke, P.M. (2016) Nanotechnology: A New Opportunity in Plant
 566 Sciences. *Trends in Plant Science* **21**: 699–712.
- 567 Wong, M.H., Misra, R.P., Giraldo, J.P., Kwak, S.-Y., Son, Y., Landry, M.P., et al. (2016) Lipid Exchange
 568 Envelope Penetration (LEEP) of Nanoparticles for Plant Engineering: A Universal Localization
 569 Mechanism. *Nano Lett* **16**: 1161–1172.

- 570 Wu, J., Du, H., Liao, X., Zhao, Y., Li, L., and Yang, L. (2011) An improved particle bombardment for the
571 generation of transgenic plants by direct immobilization of releasable Tn5 transposases onto
572 gold particles. *Plant Mol Biol* **77**: 117–127.
- 573 Zarzycki, J., Axen, S.D., Kinney, J.N., and Kerfeld, C.A. (2013) Cyanobacterial-based approaches to
574 improving photosynthesis in plants. *J Exp Bot* **64**: 787–798.
- 575 Zhai, G., Walters, K.S., Peate, D.W., Alvarez, P.J.J., and Schnoor, J.L. (2014) Transport of Gold
576 Nanoparticles through Plasmodesmata and Precipitation of Gold Ions in Woody Poplar. *Environ
577 Sci Technol Lett* **1**: 146–151.
- 578 Zhu, H., Han, J., Xiao, J.Q., and Jin, Y. (2008) Uptake, translocation, and accumulation of manufactured
579 iron oxide nanoparticles by pumpkin plants. *J Environ Monit* **10**: 713–717.
- 580 Zhu, Z.-J., Wang, H., Yan, B., Zheng, H., Jiang, Y., Miranda, O.R., et al. (2012) Effect of Surface Charge on
581 the Uptake and Distribution of Gold Nanoparticles in Four Plant Species. *Environ Sci Technol* **46**:
582 12391–12398.
583

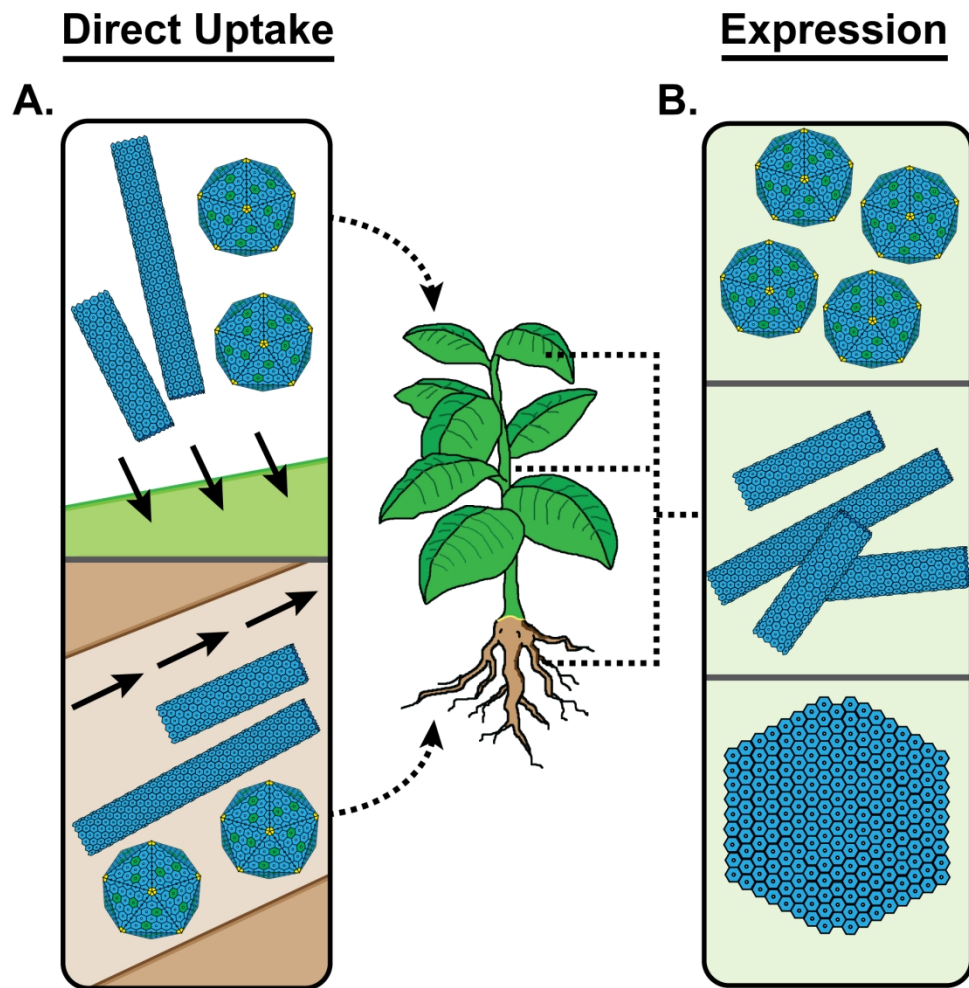


Figure 1. Direct uptake and expression of BMC-base architectures in plant systems. An overview of how BMC-based structures might be transported into and expressed within plant systems. BMC-based architectures have the potential to be used as shuttles for transporting biomaterials into plant systems or could serve a temporary purpose through transient expression in plant systems. The advantages of protein-based ENPs compared to non-biological ENPs include ease of manipulation, multifunctionality, rapid and efficient producibility, and biodegradability. A. Direct uptake of in vitro assembled BMC-based shells and nanotubes through leaves and roots. These structures have the capability to load and subsequently isolate or display cargo such as bioactive compounds, agrochemicals, and fertilizers for transport. B. Expression and assembly of encapsulating BMC shells, nanotubes, and 2D sheets in plant leaves and roots.

429x442mm (118 x 118 DPI)

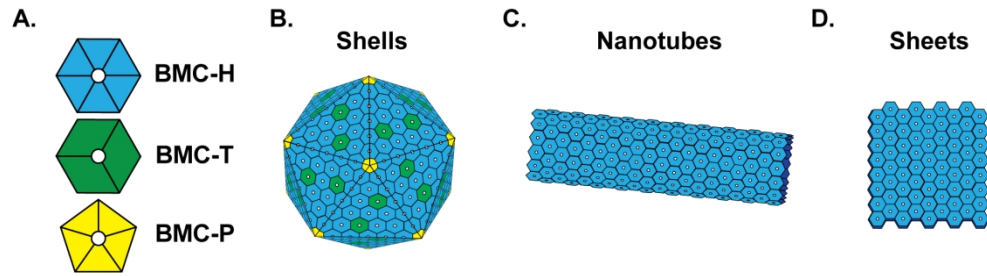


Figure 2. BMC-based components and architectures. A. Representation of BMC structural components. B. BMC shells are composed of protein hexamer (BMC-H), trimer (BMC-T), and pentamer (BMC-P) elements. The pentamers serve to cap the vertices of the protein shell. C-D. BMC-based nanotubes and sheets are composed solely of protein hexamers and pseudo-hexamers. Differences in residues along the edge periphery likely contribute to the formation of the distinct architectures.

429x119mm (118 x 118 DPI)

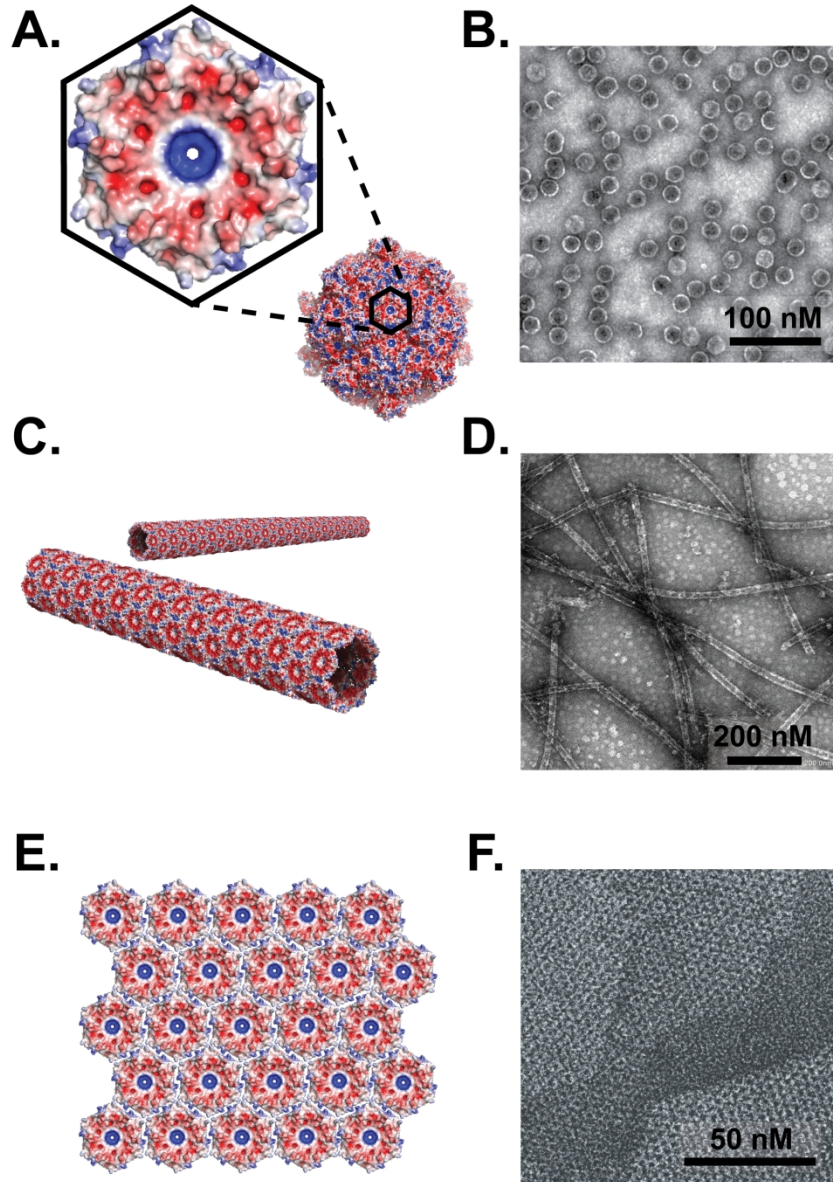


Figure 3. Models and electron microscopy images TEM of BMC-based architectures. A. Electrostatic model of synthetic beta-carboxysome shell (PDB 6OWG) with individual hexamer component outlined and (B) TEM image of minimal BMC shells on a grid. The central pore of the BMC-H and BMC-T components allow for the selective shuttling of molecules to the interior of shells. C. Electrostatic homology model of BMC-based nanotubes composed of the RmmH hexamer of *M. smegmatis* (Noël et al., 2016) and (D) TEM image of RmmH hexamer BMC-based nanotubes on a grid. E. Electrostatic representation of BMC-based sheets composed of the *H. ochraceum* BMC-H hexamer (PDB 5DJB) and (F) an unpublished TEM observation of BMC-T based sheets from *Clostridium*. BMC-based sheets have been shown in previous publications to be solely composed of BMC-H, however, as identified in this image, the pseudohexamer BMC-T can in certain cases also form sheets.

429x608mm (118 x 118 DPI)

Table 1. Nanoparticles utilized in phytonanotechnology experimentation

Nanoparticle	Size	Shape	Plant	Remarks	Ref
Liposomes	100 nm	Spherical	<i>S. lycopersicum</i>	Liposomes loaded with Fe and Mg restored acute nutrient deficiency	(Karny <i>et al.</i> , 2018)
CNTs	D x 0.8-50nm, L x 4 nm-1 um	Tube	<i>C. roseus</i> protoplasts	Penetration cell membrane and localize to nucleus, plastids, and vacuoles	(Serag <i>et al.</i> , 2011)
			<i>N. benthamiana</i>	Protection/transport of siRNA	(Demirer <i>et al.</i> , 2020)
			Soybean, barley, & wheat seeds	Penetration of seed coat	(Lahiani <i>et al.</i> , 2013)
MSNs	2-600nm	Spherical	<i>E. sativa</i> , <i>N. officinale</i> , <i>N. tabacum</i> and <i>S. oleracea</i> & <i>A. thaliana</i> protoplasts	Transport/expression of DNA through the cell membrane	(Kwak <i>et al.</i> , 2019)
			<i>N. tabacum</i>	Transportation of DNA and chemicals into isolated plant cells and intact leaves	(Torney <i>et al.</i> , 2007)
			<i>A. thaliana</i>	Delivery of foreign DNA into intact <i>A. thaliana</i> roots via direct uptake	(Chang <i>et al.</i> , 2013)
			Onion epidermis tissue	DNA delivery via gold-capped MSNs	(Martin-Ortigosa <i>et al.</i> , 2012)
AuNPs	6-50 nm	Spherical	Wheat, lupin, <i>A. thaliana</i>	Uptake and distribution during seed germination	(Hussain <i>et al.</i> , 2013)
			<i>A. thaliana</i>	AuNPs taken up by plant roots or shoots depending on charge	(Zhu <i>et al.</i> , 2012)
MagNPs	2-10nm	Spherical	<i>P. deltooides</i>	Uptake and translocation to roots, stems, and leaves	(Zhai <i>et al.</i> , 2014)
			<i>C. pepo</i>	Translocation of MagNPs in plant tissues	(González-Melendi <i>et al.</i> , 2008)
MONPs	3-200nm	Spherical	<i>A. thaliana</i>	TiO ₂ NPs Penetration of cell walls and accumulation within cell	(Kurepa <i>et al.</i> , 2010)
		Spherical	<i>T. aestivum</i>	TiO ₂ translocation and accumulation	(Larue <i>et al.</i> , 2012)
QDs	2-50nm	Spherical	<i>A. thaliana</i>	Uptake by roots and translocation to leaves	(Koo <i>et al.</i> , 2015)
			Sycamore cells	Endocytic uptake of QD particles	(Etxeberria <i>et al.</i> , 2006)